Analysis of a Coaxial-to-Waveguide Adaptor Incorporating a Dielectric Coated Probe

Marek E. Bialkowski, *Senior Member, IEEE*

Abstract—**An analysis of a coaxial-to-waveguide adaptor that incorporates a solid probe, coated with a dielectric is presented. Based on this analysis, a computer algorithm for an IBM PC is developed. The numerical results for the input impedance of the probe are presented and show good agreement with the other analyses and experiments.**

I. Introduction

ALTHOUGH there have been a number of solutions presented to the problem of modeling of a coaxial-to-waveguide adaptor [1]–[5] their use still remains limited. Analysis in [1] is not accurate enough for practical applications. On the other hand, more accurate analyses [2]–[5] are still restricted to special cases of a hollow coaxial probe [2], [5], or a solid probe [3], [4] feeding a hollow rectangular waveguide. Recently, Ansoft and Hewlett-Packard [7] have demonstrated that the analysis of a coax-to-waveguide adaptor can be performed by using a 3-D electromagnetic simulator. Since there are no restrictions on the shape and electrical parameters of the device, a variety of coax-to-waveguide adaptors can be analyzed. There is, however, one problem with this approach. In difference to [2]–[5] the general approach [7] does not include any analytical preprocessing and therefore results in time consuming calculations.

This letter reports on the modeling of a practical configuration of a coax-to-waveguide adaptor, in which the probe is solid and coated with a layer of dielectric. The method presented here includes the stage of analytical preprocessing and is computationally efficient.

II. Analysis

The device analyzed here is shown in Fig. 1. The difference from the cases considered in [2]–[5] is that the solid probe is surrounded by a cylindrical layer of dielectric. In the cylindrical region above the probe, an air or other dielectric is present.

From the designer's point of view the parameter of interest is the input impedance as seen from the coaxial aperture. This impedance is defined by [2]:

$$Z_{in} = \frac{-\int_a^b \bar{E}_a \cdot \bar{a}_r \, dr}{\frac{2\pi}{\ln\left(\frac{b}{a}\right)} \int_0^{2\pi} \int_a^b \bar{H}_a \cdot \bar{a}_\phi \, dr \, d\phi}, \tag{1}$$

where $\bar{E}_a$ is the electric field, $\bar{H}_a$ is the magnetic field present in the aperture, and r, ϕ are polar coordinates.

The magnetic field $\bar{H}_a$ can be determined once the electric field $\bar{E}_a$ in the aperture is specified. Experience shows [2], [5] that reasonably accurate results can be obtained when the electric field in the aperture $\bar{E}_a$ is approximated by the TEM coaxial field. By using this approximation the magnetic field $\bar{H}_a$ and then the input impedance of the probe can be determined through the following steps.

Step 1: The aperture is replaced by a surface magnetic current

$$\bar{M}_a = \bar{n} \times \bar{E}_a = \bar{a}_\phi \frac{V}{\ln\left(\frac{b}{a}\right)} \frac{1}{r},$$

where V is voltage between the inner and outer coaxial conductors. According to the field equivalence principle [1], $\bar{M}_a$ produces the original field $\bar{E}$, $\bar{H}$.

Step 2: Determination of the field $\bar{E}$, $\bar{H}$ is simplified by using a second form of the field equivalence principle. As shown in Fig. 2(a), two conducting cylindrical surfaces, S_1 and S_2, are introduced so that the region around the probe forms a coaxial cavity. Under these conditions the field $\bar{E}(1)$, $\bar{H}(1)$ produced in the coaxial cavity is TEM. This field has only the radial electric field component $\bar{E}r$ and the azimuthal magnetic field component $\bar{H}_\phi$.

The field $\bar{E}(1)$, $\bar{H}(1)$ induces an electric current on the walls of the cavity. The electric current Is_1, which flows along the surface S_1, is given by (2):

$$I_{s1} = -j \frac{\cos\left(k_1(y - B)\right)}{Z_c \sin\left(k_1 B\right)}, \tag{2}$$

where k_1 is a wave number, Z_c is the characteristic impedance and $j = \sqrt{-1}$. The current Is_2 which flows along the surface S_2 has the same form as (2), but it flows in the opposite direction.

Step 3: To recover the original $\bar{E}$, $\bar{H}$ field the conducting surfaces S_1 and S_2 are removed, and new electric currents Is_1' and Is_2', which are the negatives of Is_1 and Is_2, are introduced (Fig. 2(b)). In this new arrangement the magnetic current $\bar{M}_a$ is not present.

The currents Is_1' and Is_2' produce a new field $\bar{E}(2)$, $\bar{H}(2)$. The superposition of fields $\bar{E}(1)$, $\bar{H}(1)$ and $\bar{E}(2)$, $\bar{H}(2)$ gives the original field $\bar{E}$, $\bar{H}$ produced by $\bar{M}_a$ in the waveguide. The remaining task is to determine the field $\bar{E}(2)$, $\bar{H}(2)$. This is achieved in the following manner.

Manuscript received March 21, 1991.

The author is with the Department of Electrical Engineering, University of Queensland, Queensland 4072, Australia.

IEEE Log Number 9101736.

1051-8207/91/0800-0211$01.00

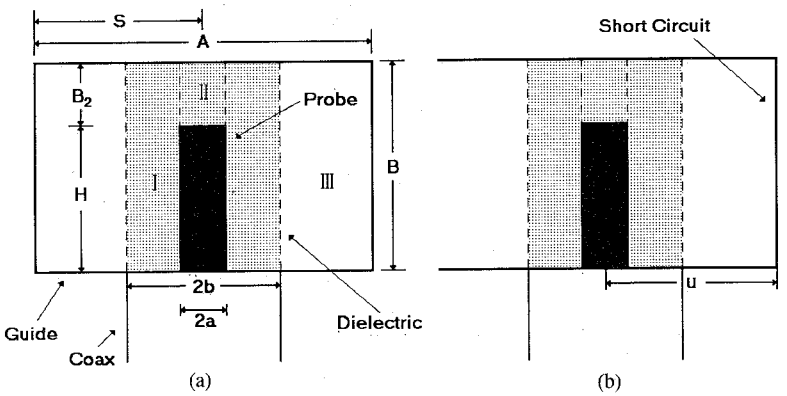

Fig. 1. Dielectric-coated solid probe antenna in a semi-infinite rectangular waveguide. (a) Cross-sectional view. (b) Side view.

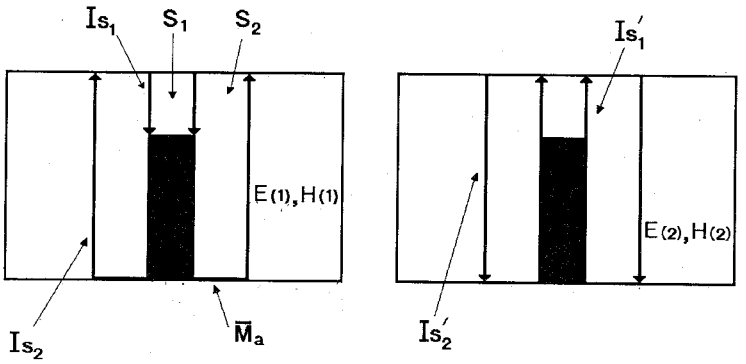

Fig. 2. Illustration of the field equivalence principle. (a) Conducting surfaces S_1 and S_2 are introduced. (b) Surfaces S_1, S_2 and magnetic current $\bar{M}_a$ are removed and electric currents I'_{s_1} and I'_{s_2} are introduced.

Step 4: The rectangular waveguide is regarded as a loaded, parallel plate, radial waveguide. Due to the form of excitation, the field $\bar{E}(2)$, $\bar{H}(2)$ can be considered as a radial TM field. The expressions for the y-component of the electric field $\bar{E}(2)$ and the ϕ-component of the magnetic field $\bar{H}(2)$ in the regions surrounding the probe can be written as follows.

For the cylindrical region, I, $a < r < b$, $0 < y < B$:

$$E_y^I = \sum_{n=0}^{M_1} \frac{\epsilon_{on}}{B} \cos\left(k_{yn} y\right)\left[A_n H_o^{(2)}\left(\Gamma_n^{(1)} r\right) + B_n J_o\left(\Gamma_n^{(1)} r\right)\right],$$

$$H_\phi^I = \sum_{n=0}^{M_1} \frac{\epsilon_{on}}{B} \frac{-jk_1}{Z_1 \Gamma_n^{(1)}} \cos\left(k_{yn} y\right) \cdot\left[A_n H_o'^{(2)}\left(\Gamma_n^{(1)} r\right) + B_n J_o'\left(\Gamma_b^{(1)} r\right)\right], \quad (3)$$

where ϵ_{on} is the Neumann factor, Z_1 is an intrinsic impedance, $k_{yn} = n\pi/B$, $\Gamma_n^{(1)2} = k_1^2 - k_{yn}^2$, Jo is a Bessel function $Ho^{(2)}$ is a Hankel function, Jo' and Ho' are their derivatives, and An, Bn are unknown expansion coefficients.

Similarly for the cylindrical region II, $0 < r < a$, $H < y < B$:

$$E_y^{II} = \sum_{n=0}^{M_2} \frac{\epsilon_{on}}{B_2} \cos\left(k_{yn}^{(2)}(y - H)\right) C_n J_o\left(\Gamma_n^{(2)} r\right),$$

$$H_\phi^{II} = \sum_{n=0}^{M_2} \frac{\epsilon_{on}}{B_2} \frac{-jk_2}{Z_2 \Gamma_n^{(2)}} \cos\left(k_{yn}^{(2)}(y - H)\right) C_n J_o'\left(\Gamma_n^{(2)} r\right), \quad (4)$$

where k_2 is a wave number, Z_2 is an intrinsic impedance, $H = B - B_2$ is the probe height, $k_{yn}^{(2)} = n\pi/B_2$, $\Gamma_n^{(2)2} = k_2^2 - k_{yn}^{(2)2}$, and Cn are unknown expansion coefficients.

The field at the boundary $r = b$ can be represented in the form

$$E_y^{III} = \sum_{n=0}^{M_3} F_n \frac{\epsilon_{on}}{B} \cos k_{yn} y,$$

$$H_\phi^{III} = \sum_{n=0}^{M_3} F_n \frac{\epsilon_{on}}{B} \frac{-jk_3}{3_n \Gamma_n^{(3)}} \cos\left(k_{yn} y\right) \frac{H_0'^{(2)}\left(\Gamma_n^{(3)} b\right)}{H_o^{(2)}\left(\Gamma_n^{(3)} b\right)}, \quad (5)$$

where k_3 is a wave number, $\Gamma_n^{(3)2} = k_3^2 - k_{yn}^2$, $3n$ is the impedance of the nth TM radial harmonic, and Fn are unknown expansion coefficients.

Defined in (5), impedance $3n$ takes into account the presence of waveguide side walls and a short. The method for determining its value has been explained in [6]. In that

method, $3n$ is given by a rapidly converging series, which is easily implemented in the form of a short computer algorithm.

The unknown expansion coefficients An, Bn, Cn, Fn in (3), (4), (5) can be determined by applying the boundary conditions:

At $r = a$,

$$E_y^I = \begin{cases} E_y^{II}, & \text{for } H \le y \le B, \\ 0, & \text{for } 0 \le y \le H, \end{cases}$$

$$H_\phi^I = H_\phi^{II}, \qquad \text{for } H \le y \le B,$$

At $r = b$,

$$E_y^I = E_y^{III}$$
$$H_\phi^I = H_\phi^{III}, \qquad \text{for } 0 \le y \le B. \tag{6}$$

By applying a Fourier analysis, (6) can be converted into a system of linear algebraic equations. The unknowns An, Bn, and Fn can be expressed in terms of unknowns Cn. The resulting system of equations for unknowns Cn can be easily solved.

By having determined coefficients Cn, An, Bn, and Fn the fields $\bar{E}(2)$, $\bar{H}(2)$ in all the individual regions are known through the use of (3), (4), (5).

Step 5: Assuming that the field $\bar{E}$, $\bar{H}$ is known in cylindrical region I, the input admittance of the coaxial probe can be determined by using (1) and is given by (7):

$$Y_{in} = Y_{in_{\text{TEM}}} + Y_{in_{\text{TM}}}, \tag{7}$$

where

$$Y_{in_{\text{TEM}}} = -j\frac{\cot(k_1 B)}{Z_c},$$

$$Y_{in_{\text{TM}}} = \frac{-jk_1}{Z_c B}\sum_{n=0}^{M_1}\frac{\epsilon_{on}}{\Gamma_n^{(1)^2}}\left\{A_n\left[H_o^{(2)}(\Gamma_n^{(1)}b) - H_o^{(2)}(\Gamma_n^{(1)}a)\right] + B_n\left[J_o(\Gamma_n^{(1)}b) - J_o(\Gamma_n^{(1)}a)\right]\right.,$$

represent the TEM and TM contributions.

III. Extension for a Double Dielectric Coating

The theoretical analysis of the coax-to-waveguide adaptor previously described can be extended to the case of a double layer of dielectric surrounding the probe. In this arrangement the second layer extends for $r: b < r < c$. This new degree of freedom can be of importance for metal coated dielectric waveguides with a cylindrical air gap between the probe and the dielectric filling the guide. The extension of the analysis for the new case is straight forward, but is not described here.

IV. Results

Based on the theoretical analysis described, a computer algorithm in Fortran for an IBM PC/AT or compatible has been developed.

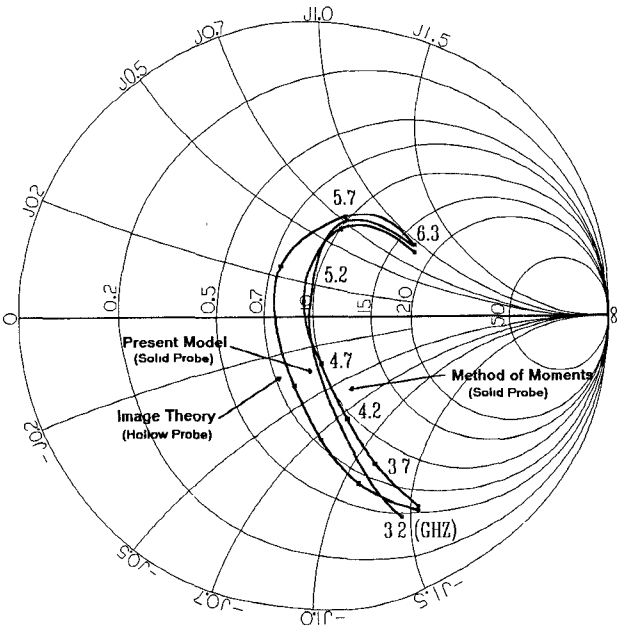

Fig. 3. Comparison between different numerical results for the input impedance of the coaxial probe. Waveguide and probe dimensions: a = 0.635 mm, b = 2.12 mm, H = 14.4 mm, A = 57.04 mm, B = 28.8 mm, u = 19.2 mm. Probe is positioned at the center of the waveguide. Relative permittivity for all regions in the waveguide: 1.

The algorithm could be easily tested for the cases of an uncoated probe that were presented in [2]–[5]. Fig. 3 shows a comparison between the results obtained for a solid probe by using the newly developed algorithm with those obtained by using the method of moments [3]. Also included are results obtained by using the method of images for the hollow probe [2].

The results obtained with the new algorithm agree well with those produced by the method of moments. A slight discrepancy can probably be explained by different definitions of the input impedance. The impedance in [3] was calculated as the ratio of voltage to current. It can be seen that there is a discrepancy between the results for the input impedance for a hollow and a solid probe. For example, the results for the solid probe show a good impedance match at about 5.2 GHz. This is not the case for the hollow probe.

In order to investigate the case of a coated probe, the analysis of a popular Hewlett-Packard coaxial-to-waveguide adaptor, the X281A, was performed. Fig. 4 shows the results for the input impedance of the probe as seen at the coaxial aperture, for a frequency band from 8.2 to 12.4 GHz. The maximum SWR in the band 8.5–12.4 GHz is 1.25 and it rises to 1.38 at 8.2 GHz. These results agree well with the manufacturer's specifications: maximum SWR of 1.25 for the frequency range 8.2–12.4 GHz.

It should be noted that the X281A adaptor also incorporates an additional coaxial matching circuit, which probably further reduces any mismatch. The coaxial matching circuit has not been taken into account during calculations. It is worth mentioning that it only took a few seconds of CPU time of IBM PC to produce the results for the input impedance shown in Figs. 3 and 4.

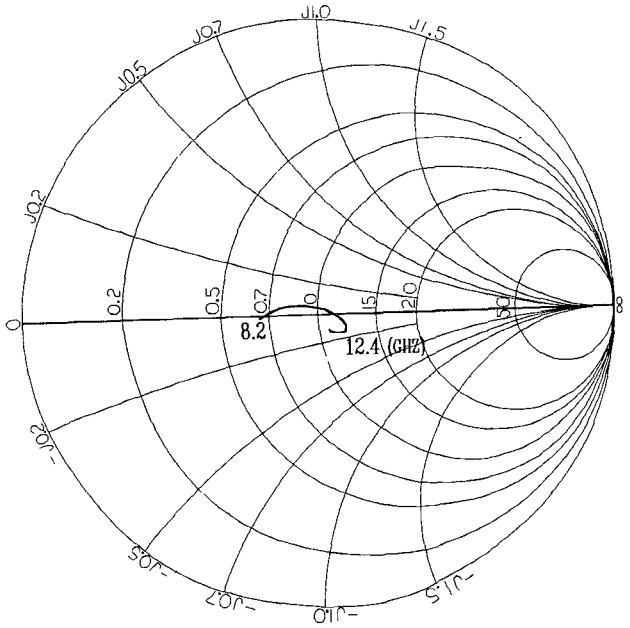

Fig. 4. Numerical results for the input impedance of the X281A coaxial adaptor. Waveguide and probe dimensions: $a = 0.55$ mm, $b = 2.5$ mm, $H = 4.5$ mm, $A = 22.86$ mm, $B = 10.16$ mm, $u = 5.1$ mm. Probe positioned centrally. Relative permittivity for regions I and II: 2.4. Relative permittivity for the waveguide region III: 1.

Conclusion

The analysis of a coaxial-to-waveguide adaptor with a dielectric-coated solid probe has been presented. Based on this analysis a computer algorithm has been developed.

This algorithm has been verified and shows good agreement with other algorithms and experiments. The presented analysis and the developed computer algorithm should be of help to the designers of coax-to-waveguide adaptors.

References

[1] R. E. Collin, *Field Theory of Guided Waves*. New York: McGraw-Hill, 1960, pp. 258–271.

[2] A. G. Williamson, "Coaxially fed, hollow probe in a rectangular waveguide," *Proc. Inst. Elect. Eng.*, vol. 132, pt. H, pp. 273–285, 1985.

[3] J. M. Jarem, "A multifilament method of moments solution for the input impedance of a probe-excited semi-infinite waveguide," *IEEE Trans. Microwave Theory Tech.*, vol. MTT-35, no. 1, pp. 14–19, Jan. 1987.

[4] J. M. Rollins and J. M. Jarem, "The input impedance of a hollow-probe-fed, semi-infinite rectangular waveguide," *IEEE Trans. Microwave Theory Tech.*, vol. MTT-37, no. 7, pp. 1144–46, July 1989.

[5] M. E. Bialkowski, "Probe antenna in arbitrarily terminated rectangular waveguide," *Archiv für Elektronik, AEU*, vol. 39, no. 3, pp. 190–193, 1985.

[6] ——, "Analysis of disc-type resonator mounts in parallel plate and rectangular waveguides," *Archiv für Elektronik, AEU*, vol. 38, no. 5, pp. 306–311, 1984.

[7] A. Anger, "Software computes Maxwell's equations," *Microwave J.*, vol. 33, no. 2, Feb. 1990.